Monitoring Uniform Corrosion of Storage Tank Bottom Steel by Acoustic Emission technique

Haisheng Bi[1,], Dedong Hu[1], Zili Li[2], Qingwei Niu[2], Isaac Toku-Gyamerah[2], Jianfei Chen[3]*

[1]College of Electromechanical Engineering, Qingdao University of Science & Technology, Qingdao, Shandong, 266042, China
[2]College of Pipeline and Civil Engineering, China University of Petroleum, Qingdao, Shandong, 266580, China
[3] Shengli Oilfield Technical Test Center, SINOPEC, Dongying, Shandong, 257000, China
[*]E-mail: haishengbicup@gmail.com

Measurements of uniform corrosion of atmospheric metal storage tank bottom steel specimens by acoustic emission (AE) and electrochemical methods were carried out simultaneously in diluted sulfuric acid (H_2SO_4) solution (pH=4.5). The potentiostatic polarization measurements indicated that AE activity was positive correlation with the corrosion level. AE signal generated from uniform corrosion was analyzed by characteristic parameters in time domain and spectrum in frequency domain respectively, and further time-frequency local analysis was presented using the Gabor Wavelet transform (WT). The result shows that the AE technique is very sensitive to tank bottom steel uniform corrosion, corrosion products' deposits and movement, so that AE activity can be used to represent the corrosion rate. These conclusions will be helpful for explaining and evaluating the on-site storage tank bottom AE testing result.

1. INTRODUCTION

Corrosion is one of the main causes of catastrophes to structures and equipment in petrochemical industries. Atmospheric storage tanks, heavy pressure vessels, pipelines, phase separators, heat exchangers and much other industrial equipment gradually corroded by electrochemical reactions within their environment. The most common types of corrosion are pitting and uniform corrosion[1]. The atmospheric storage tanks play an irreplaceable role in storage and transportation of crude oil and oil derivatives. However, tank bottom corrosion has been recognized as

a potential threat to storage tank security all over the world. This can cause very serious consequences on the environment, health and safety, producing a very wide range of hazards and disasters. Therefore, the storage tank bottom corrosion has attracted more and more attentions in recent decades [2-5].

The storage tank bottom corrosion damage is a very complicated process [6, 7]. The sedimentary water at the tank bottom contaminated by several corrosive ions can induce uniform corrosion in the whole bottom plates, causing the plate thickness losses and even large area deformation. Hence, periodic internal inspection is necessary to prevent destruction from tank bottom corrosion according to API 581 and 653 standards. Several conventional testing techniques such as magnetic flux leakage (MFL) testing and remote field eddy current testing (RFECT) have been applied to detect and locate the defects [8-11]. However, these techniques often result in expensive and time-consuming to clear and inspect the tank, which can influence the normal production. If the tank bottom without severe corrosion, internal inspection will cause unnecessary inspection cost and business interruption loss. Therefore, cost-effective and on-line diagnosis techniques are increasingly needed for detecting and evaluating dynamic defects of storage tanks bottom. The acoustic emission is considered to meet the requirements of an on-line inspection and has gained popularity [12-17].

Acoustic emission is a non-destructive technique (NDT), defined as the phenomena whereby transient elastic waves are generated by the rapid release of energy from localized sources within a material, also known as the stress wave emission or micro-seismic activity. It is widely used to detect and monitor the process of plastic yield deformation, fatigue fracture, stress cracking and corrosion damage. Extracting and analyzing the effective signal to evaluate the features of AE sources is the bottleneck to AE on-site inspection. Previous research has shown that the AE activity is closely related to corrosion types and corrosion rate [18-20]. Prateepasen et al. observed the hydrogen evolution, oscillation and bubble burst AE signal from growing pits [21, 22], similar results were also got in Cakir and co-workers' work. However, Magaino et al. postulated that the AE signal was mainly released from transient stress change on the metal surface. Darowicki et al. [23, 24] obtained the pitting corrosion potential of aluminum through the cumulative distribution function of the probability of pitting corrosion occurrence on the basis of AE data. Ferrer and Idrissi [25-27] studied the abrasion-corrosion transition of austenitic stainless and propose a few hypotheses based on the effect of abrasion on the corrosion and the effect of corrosion on the abrasion. Compared to the AE research on pitting corrosion of stainless steel and aluminum alloy, few papers were focused on uniform corrosion of tank bottom steel. Yuyama and Kitsukawa [28-30] presented a method to predict the tank bottom corrosion severity by correlation between AE activity and corrosion risk parameter. Fregonese and Jaubert [31] monitored the rubber coating of storage tank bottom using AE and electrochemical technique. In that context, the purpose of the present study is to extract the features of AE signals during uniform corrosion of storage tank bottom steel.

2. EXPERIMENTAL PROCEDURE

2.1. Material

Specimens were cut out of steel sheets from the replacement storage tank bottom plates of industrial tanks, their sizes are 29mm × 29mm. Composition of steel (1.9-2.1mm) is given in Table 1. The working surface was polished with a series of silicon carbide (SiC) sheets of up to 1200 grit, and the other surface was polished with 800 SiC paper grade to ensure a good AE sensor coupling. The specimens were rinsed with de-ionized (DI) water then acetone and alcohol, after that they were dried in a desiccator, and weighted, labeled and stored to be used.

Table 1. Composition of the tank bottom steel

Element	Fe	C	Si	Mn	P	S
Wt.%	Balance	0.170	0.300	0.610	0.050	0.045

2.2. Experimental device

The experiments were conducted in a diluted sulfuric acid solution with pH adjusted to 4.5 at room temperature. The size of the electrolytic cell is $25 \times 25 \times 25$ cm^3, and it is made of transparent organic glass to avoid producing other corrosion signal. The specimen was sealed by epoxy resin and inserted in the center hole of the electrolytic cell bottom, and the edges of the hole were filled with silicone sealant to ensure no leakage (see Figure 1). An AE sensor was mounted on the back of the specimen by the acoustic couplant Vaseline for real-time monitoring corrosion signals and connected to the AMSY-5 data acquisition channel. There are rubber cushions between the container bottom and the base stents, also the base stents and lab table to reduce external vibration. The electrochemical measurements were conducted simultaneously to confirm the result of acoustic emission detection.
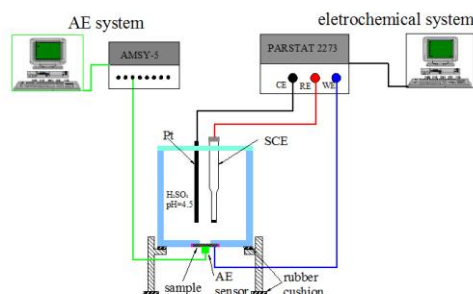

Figure 1. Schematic diagram of experiment system

2.3. Electrochemical measurements

Electrochemical measurements were carried out with a PAR 2273 potentiostat and the PowerSuite software. The minimum current resolution of system is 1.2 fA and the minimum potential

step is 2.5 µV. An electrochemical cell with a typical three-electrode configuration was used. The sample used as the working electrode (WE), its electrochemical potential was measured with a saturated calomel (SCE) reference electrode (RE) and a platinum plate as the counter electrode (CE).

2.4. Acoustic Emission monitoring

AE instrumentation consisted of a piezoelectric sensor (VS30-SIC type from Vallen, integral preamplifier: 46 dB gain) and an acquisition system AMSY-5 from Germany Vallen-Systeme GmbH, the AMSY-5 is a fully digital multi-channel AE system. The AE sensor and its frequency response curve are shown in Figure 2. AE acquisition threshold was fixed at 30.2 dB according to background noise level. Other acquisition parameters setting are shown in Table 2.
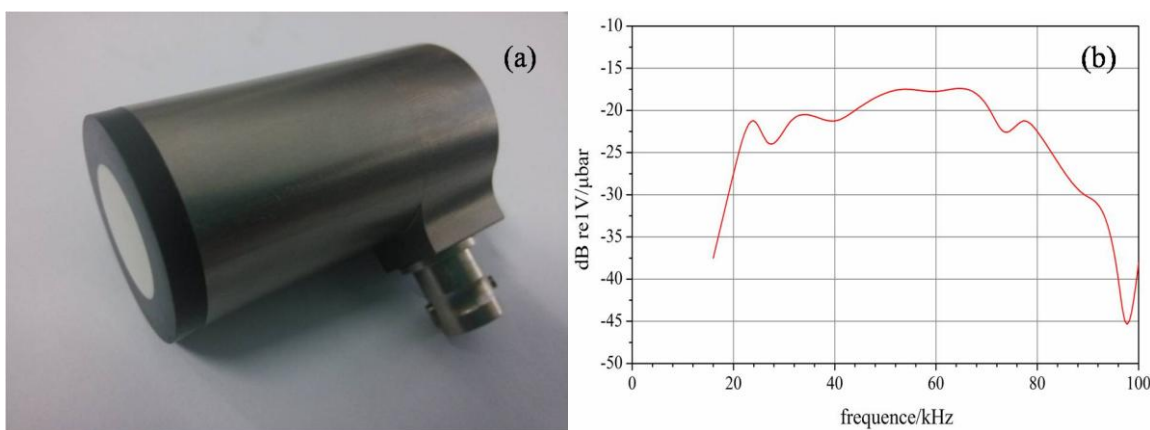

Figure 2. AE sensor and the frequency response curve (a) VS30-SIC-46dB sensor and (b) Frequency response curve

Table 2. AE acquisition parameter setting

Threshold /dB	Calc. gain /dB	Filter bandwidth /kHz	Sample rate /MHz	Sampling Number	Duration discr. time /µs	Rearm time /ms
30.2	46	25-300	2	8192	250	1.0

3. RESULTS AND DISCUSSION

The corrosive solution was filled into the electrochemical cell at 80% of the container's height, standing for at least 2h to stabilize the open circuit potential (OCP). Then the Tafel polarization measurements of 1#-3# specimens were performed with a potential sweep ranged between -250mV vs.OCP and +250mV vs.OCP, and with a scan rate of 0.167 mV/s. The corrosion potential (E_{corr}) was determined from the intersection of the Tafel lines of the polarization curve was shown in Figure 3.

The average E_{corr} is about -0.538 V (vs.SCE) by Tafel fit. The potentiostatic polarization test was performed at E_{corr} for 5h and corrosion AE signals were acquired simultaneously.
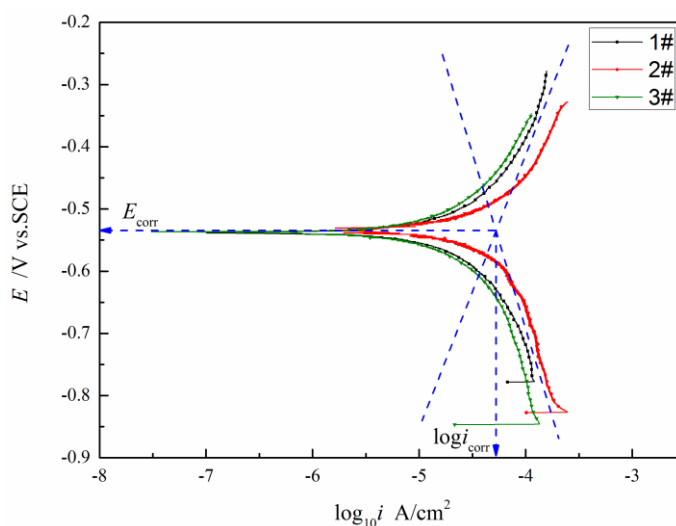

Figure 3. The polarization curves of Q235 steel of uniform corrosion in H_2SO_4 solution, pH 4.5

3.1 Corrosion AE signal analysis based on characteristic parameters

The cumulative AE hits change with time in the uniform corrosion process was shown in Figure 4. The ratio of the cumulative AE hits to the acquisition time is defined as average AE hit rate. The slope of the curve in Figure 4 can represent the average AE hit rate. It showed that there existed three different stages in the corrosion process obviously. Before 4000s, called stage I, it calculated that the average AE hit rate was about 0.06 hit/s. The AE activity generated by corrosion was in a relatively low level, and the uniform corrosion on the sample was not obvious. From 4000s to 10000s, AE hit number increased rapidly, and the hit rate reached 0.10 hit/s. The AE activity enhanced significantly, it indicated that the corrosion of the sample became more severe. In the stage III, the hit rate sharply decreased to 0.01 hit/s, this value was only one in ten corresponding to the stage II. Previous research had shown that the AE activity was closely related to the corrosion degree. In the experiments, only some random distribution corrosion spots were observed in the first stage. In the second stage, uniform corrosion had expanded to the whole surface of the sample, and a thin corrosion product film was formed gradually. The main formation of corrosion products are ferrous oxide (Fe_3O_4) and ferric oxide (Fe_2O_3) [28, 32-34], according to corrosion process, the corrosion products layer grows up and their volume expansion give rise to cracking under a certain condition. The movements and cracking of the corrosion products generated large amount of AE signals. When the surface was covered by corrosion product film completely in the last stage, the metal matrix was separated from the solution by the film which hindered the metal dissolved to metal ions into the solution. Many researchers have proved that the corrosion products Fe_3O_4 and Fe_2O_3 act as a barrier protecting the steel from further corrosion. However, this film is not permanently maintained as protective similar to $FeCO_3$ film [35, 36] in carbon dioxide corrosion of low carbon steel. In this study, in spite of the corrosion product film was not long-lasting film, the AE activity really reduced greatly for its temporary protective ability.
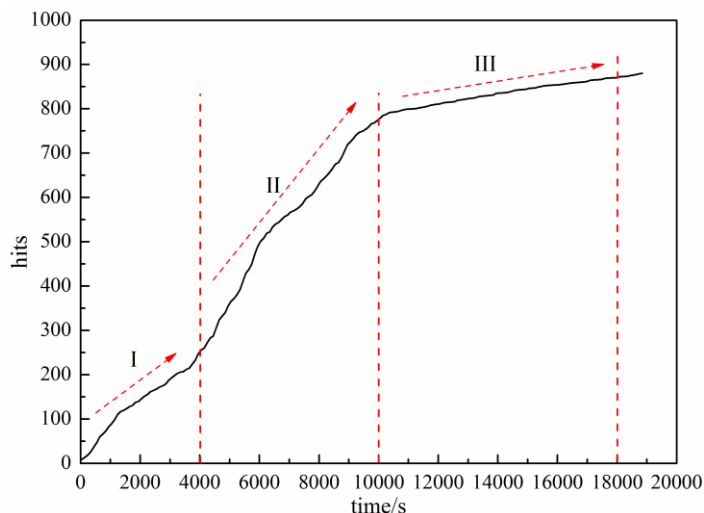
Figure 4. AE hits accumulate with time

AE signal energy most directly indicates the activity of the AE source. The change of the AE energy reflects the energy released from corrosion activity, that is to say it reflects the corrosion level. As shown in Figure 5, cumulative AE energy change with time was similar to the change of AE hit rate. The accumulative energy increase range in each stage was different obviously. It showed that the AE changes of stage I, II and III were corresponding to the process of the initial corrosion, general corrosion and corrosion decrease of the tank bottom steel.
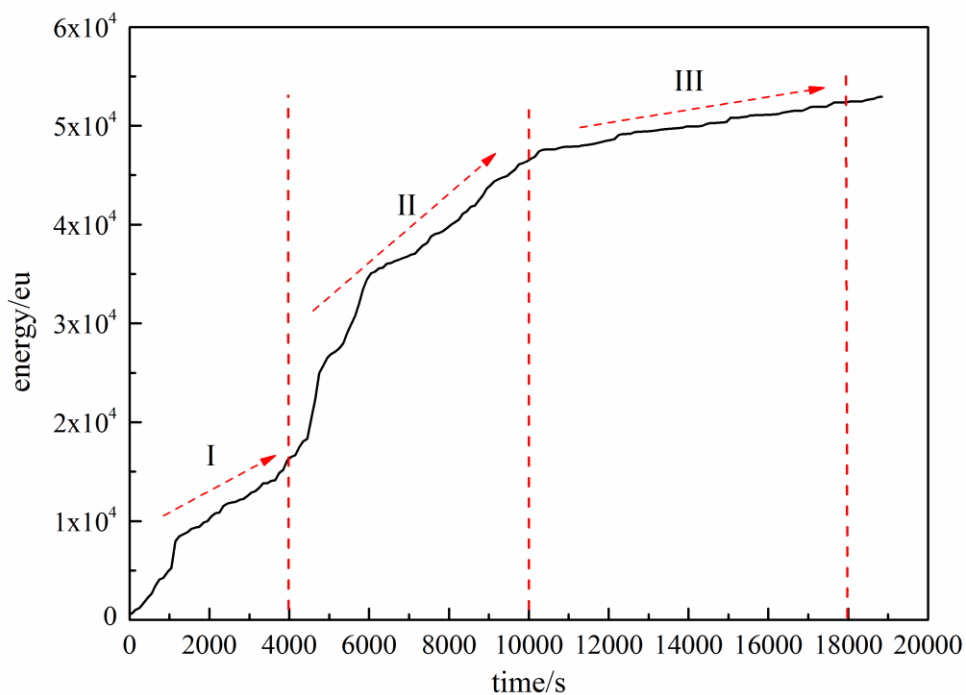

Figure 5. AE energy accumulate with time ($1eu=10^{-14}$ V^2s)
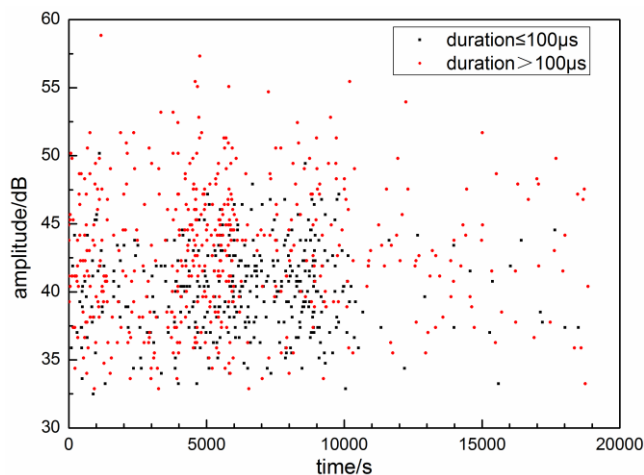
Figure 6. AE signal amplitude distribution with time

The AE signal amplitude distribution with time was shown in Figure 6. Large amount of high duration AE signals were captured from 4000 to 10000 s, and the amplitude concentrated distributed ranging from 32.5 to 52.5dB. It showed that AE signal with short duration (≤100μs) took dominant, while signal with long duration (>100μs) had higher amplitude. It indicated that AE signal mainly generated by uniform corrosion, accompanied with the movement and the friction of the corrosion products. After 10000s, the AE signal decreased dramatically, and AE intensity also reduced, most of the signals duration was over 100μs. Because of the corrosion product films protective ability, most of the AE signals mainly generated by corrosion product activity in the last stage.
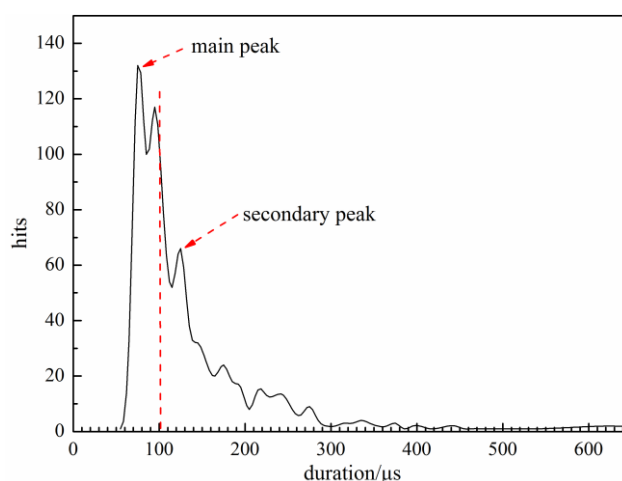

Figure 7. AE hits distribution with duration

In order to confirm the above conclusions, the correlation of AE parameters between hits and duration was illustrated in Figure 7. The hit peak value corresponding to the duration was about 70μs, and a large proportion of hits with duration below 100μs. The second hit peak corresponding to the duration was around 130μs. It illustrated that the duration of the dominant AE signal generated by uniform corrosion was shorter than the AE signals released from corrosion product activity.

3.2 Corrosion AE signal analysis based on spectrum analysis

In order to further extract the features of two dominated types of AE signal in uniform corrosion process, these two types of AE signal was analysis by waveform in the time domain and spectrum in the frequency domain. AE signal with duration above 100μs and duration below 100μs were done Fourier transform respectively.
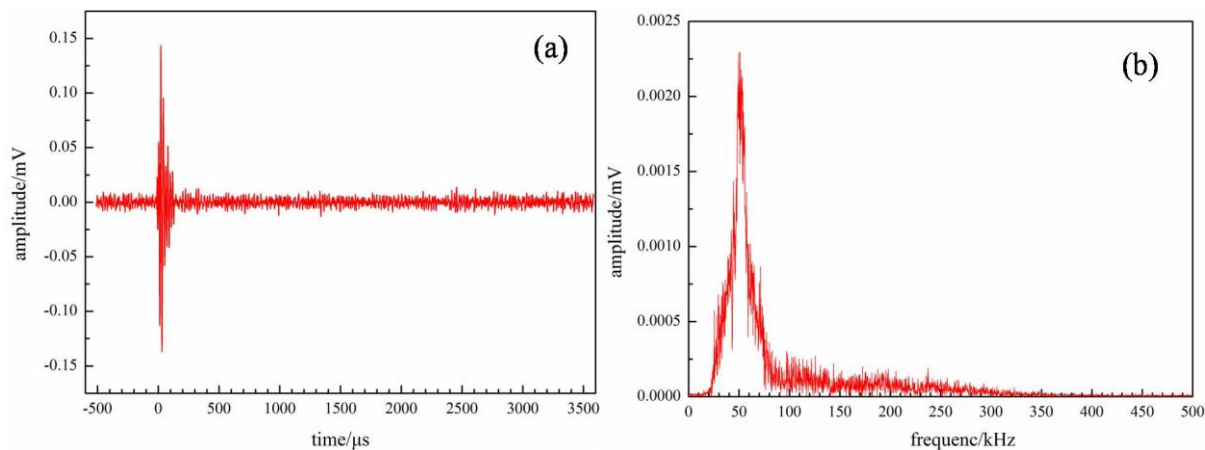

Figure 8. AE hits' waveform and average frequency spectrum of uniform corrosion (a) waveform and (b) average frequency spectrum
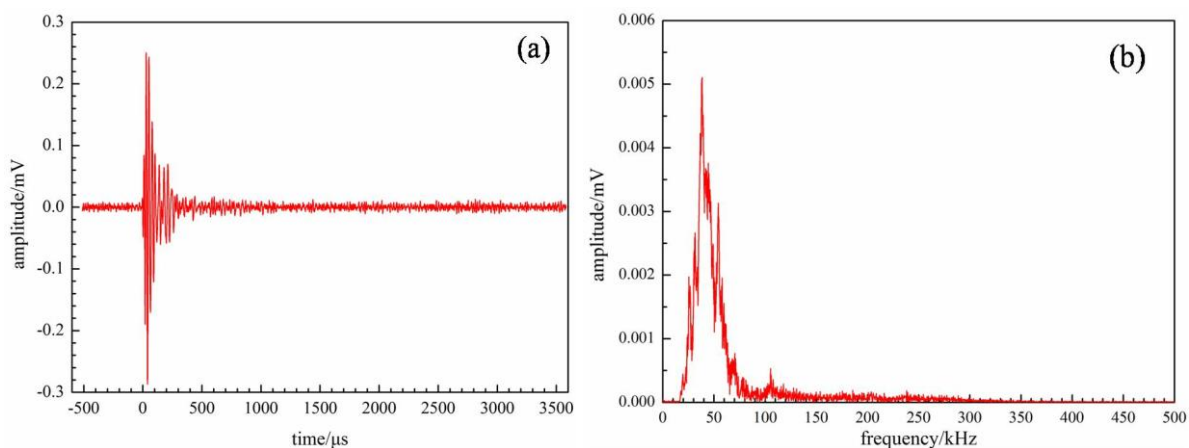

Figure 9. AE hits' waveform and average frequency spectrum of movement of corrosion products (a) waveform and (b) average frequency spectrum

Then all the AE hits' frequency spectrum in each group were used to calculate the average spectrum according to Eq.(1)

$$\hat{f}(\omega) = \frac{\sum\limits_{i=1}^{N} \int\limits_{0}^{T} f(t)e^{-j\omega t}\,\mathrm{d}t}{N} \qquad (1)$$

After calculated the average spectrum by Eq.(1), and then the average spectrum was converted to time domain waveform by the inverse Fourier transform according to Eq.(2)

$$f(t) = \frac{1}{2\pi} \int_{-\infty}^{\infty} \hat{f}(\omega) e^{j\omega t} d\omega \qquad (2)$$

Where, N is the number of the AE hits in each group. The average frequency spectrum and the time domain waveform of the two types were shown in Figure 8 and Figure 9.

As can be seen from Figure 8 and Figure 9, there was slightly different between the two types of the signal frequency spectrum, AE signal amplitude generated from uniform corrosion was approximately 0.15mV, the frequency band ranged from 30 to 60 kHz, the peak frequency was about 50 kHz; While the AE signal amplitude released from corrosion product activity was about 0.28mV, and the peak frequency and frequency range were similar to the former. These indicated that uniform corrosion of tank bottom steel mainly generated abundant low-frequency AE signals, and the frequency was mainly concentrated in the range of 30 ~ 60 kHz.

3.3 Corrosion AE signal based on wavelet transform

As is known that the traditional Fast Fourier transform (FFT) in the time domain has none positioning capability, and it can't express the local feature of the signal in the time-frequency domain. While wavelet analysis is a kind of time-frequency domain analysis, it overcomes all of these inadequate and has a strong ability in the time-frequency localization analysis. Corrosion AE signal is often considered as random non-stationary AE signal, FFT can't process this kind of signal well. Therefore, wavelet analysis is used to extract the AE signal features during corrosion process, and identify different types of corrosion AE sources.

Wavelet transform (WT) with different wavelet functions was applied to process signals in previous work, wavelets such as Haar, Coiflet, Symmlet, Gaussian or Daubechies [37-39], in spite of the results were essentially the same, differences still existed when processing different signals employed different wavelets. In our study, Gabor wavelet based on Gaussian function choice was made, because it is suited to the AE phenomena and the scale-frequency correspondence is provided [40, 41], Gabor WT has a better time-frequency resolution, and its function $\psi_g(t)$ is given as:

$$\psi_g(t) = \frac{1}{\sqrt[4]{\pi}} \sqrt{\frac{\omega_0}{\gamma}} \exp\left[-\frac{(\omega_0/\gamma)^2}{2} t^2\right] \exp(j\omega_0 t) \qquad (3)$$

And its Fourier transform $\hat{\psi}_g(\omega)$ is given as:

$$\hat{\psi}_g(\omega) = \frac{\sqrt{2\pi}}{\sqrt[4]{\pi}} \sqrt{\frac{\gamma}{\omega_0}} \exp\left[-\frac{(\gamma/\omega_0)^2}{2}(\omega - \omega_0)^2\right] \qquad (4)$$

Where, t is time, ω_0 is the center frequency of the signal, and γ is a constant taken as $\gamma = \pi\sqrt{2/\ln 2} = 5.336$. From the Gabor wavelet transform, the half-value frequency width to be $\frac{2\omega_0}{\gamma}$, and half value-time width to be $\frac{2\gamma}{\omega_0}$.
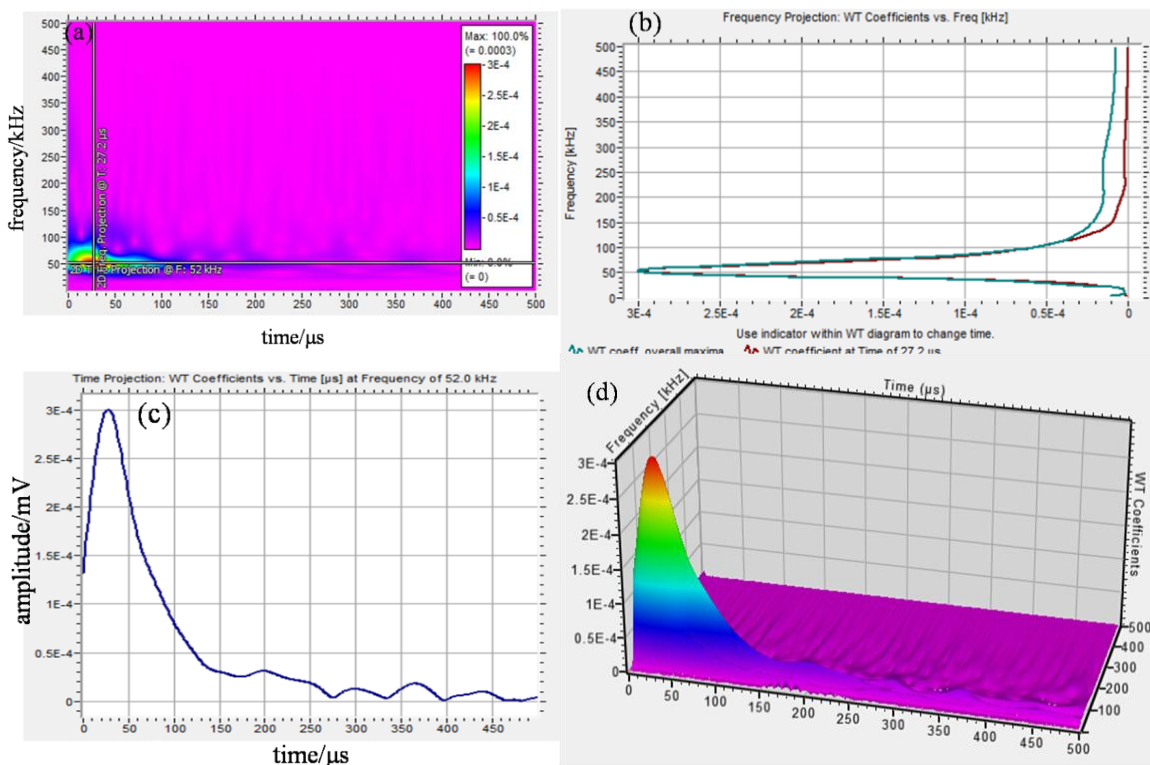
Figure 10. Gabor WT coefficients diagram of uniform corrosion AE signal (a) 2D time-frequency plane (b) 2D frequency projection (c) 2D time projection and (d) 3D time- frequency map
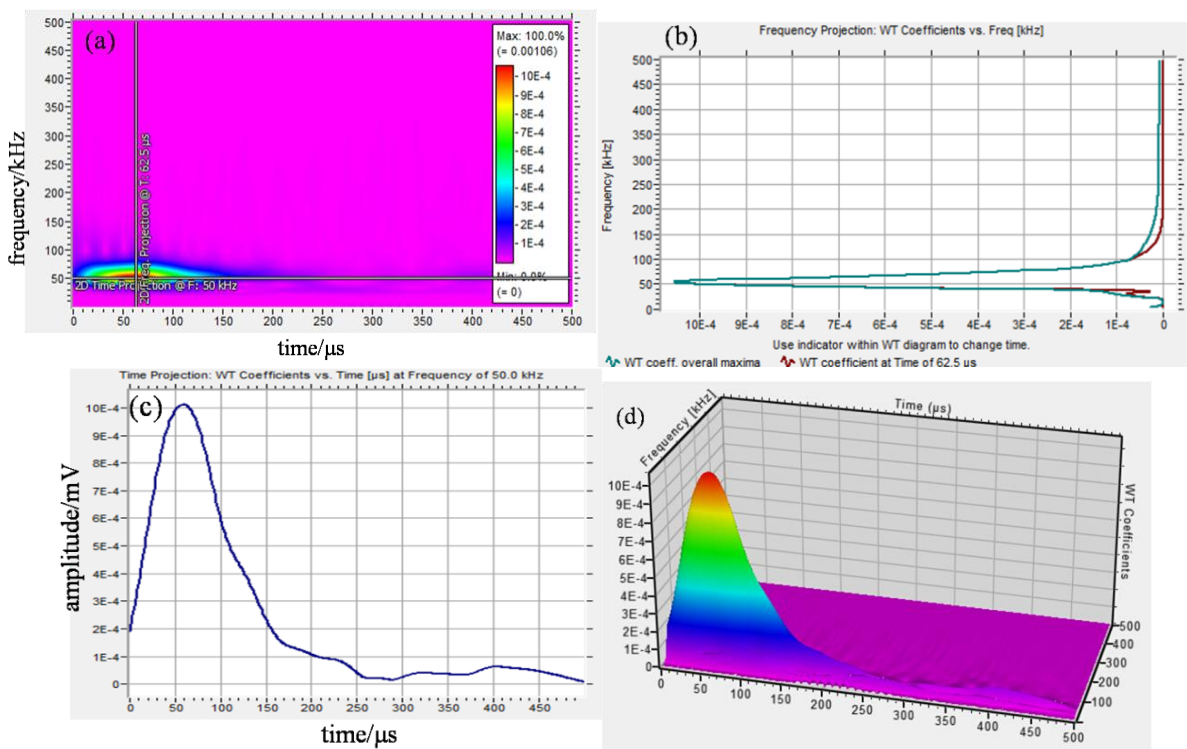

Figure11. Gabor WT coefficients diagram of corrosion product movement AE signal (a) 2D time-frequency plane (b) 2D frequency projection (c) 2D time projection and (d) 3D time-frequency map

The Gabor WT analysis of the two types of AE signals during corrosion process was described in Figure 10 and Figure 11.

Gabor Wavelet analysis of AE signal generated by uniform corrosion was shown in Figure 10 (a). The rainbow colors in the wavelet transform encode the magnitudes of the wavelet transform. It represents the energy of signal frequency component at some point in a certain time (red represents the maximum value, pink represents the minimum value). Find the maximum wavelet transform coefficients point from the time-frequency plane to get the AE signal feature. Do time slice perpendicular to the time axis passing through the points (frequency projection) and perpendicular to the frequency axis (time projection) respectively. Figure 10 (b) was the time slice at 27.2μs, it showed that the signal energy concentrated in the low frequency ranged from 25 kHz to 70 kHz, and the peak frequency was 52 kHz; Corresponding to the frequency slices in Figure 10 (c), maximum amplitude emerged at 27.2μs, the signal duration was below 80μs; The time-frequency domain local distribution feature of signal energy could be more visually seen from 3D map after Gabor WT (see Figure 10(d)). Similarly, the same analysis was performed for AE signal generated by corrosion products activity shown in Figure 11(a-d). It found that two types of signals were similar in the frequency domain, both the peak frequency appeared around 50 kHz, and the signal took overwhelmingly dominant at low frequency ranging from 25 kHz to 70 kHz. In the time domain, it showed that the maximum amplitude of the later emerged at 62.5μs, it lagged behind the former by 35μs, and its duration was relatively longer. Gabor WT results accurately reflected the energy features concentrated near the peak frequency, it was further illustrated that the low-frequency AE signals with peak frequency at 50 kHz were the main signal generated by uniform corrosion of the tank bottom steel.

4. CONCLUSIONS

This work aimed at investigating uniform corrosion of storage tank bottom steel using the AE and potentiostatic polarization methods, and the following conclusions can be obtained:

1. In the uniform corrosion process of tank bottom steel, the level of AE activity and the AE intensity are closely related to the extent of corrosion, and AE hit rate can represent the corrosion rate to some extent.

2. Uniform corrosion and corrosion product activity can generate significantly AE signal, the signal amplitude is concentrated in the range from 32 dB to 55 dB. The two types of AE signal can be distinguished by the "duration time", uniform corrosion AE duration is substantially below 100μs, while the corrosion product activity AE duration is relatively longer.

3. Abundant low-frequency AE signals were generated in the uniform corrosion process, the signal frequency mainly ranges between 25 kHz and 70 kHz, and the peak frequency is about 50 kHz.

Center, Sinopec, China for AMSY-5 device and the German Vallen-Systeme GmbH for AGU-Vallen Wavelet software.

Reference

1. F. Liu, X. Guo, D. Hu, W. Guo and N. Jin, *Nondestruct. Test. Eva.,* 25 (2010) 45
2. K. C. Garrity and P. D. Simon, *Mater. Performance*, 45 (2006) 18
3. J. Shuai, K. Han and X. Xu, *J. Loss. Prevent. Proc.*, 25 (2012) 166
4. S. B. Ding, F. J. Liu, Y. T. Xu and X. L. Guo, *Pres Ves P* (2009) 509
5. W. H. Guan, Y. H. Tao, X. D. Chen, R. Yuan and Y. F. Chen, *Proceedings of the Asme Pressure Vessels and Piping Conference 2007, Vol 5* (2008) 151
6. Y. Zhou, M. Liu, X. Ni, D. Chen and W. Wei, *Advanced Materials research,* 317-319 (2011) 66
7. A. Zagorski, H. Matysiak, O. Tsyrulnyk, O. Zvirko, H. Nykyforchyn and K. Kurzydlowski, *Mater. Sci.*, 40 (2004) 421
8. A. R. Ramirez, J. S. D. Mason and N. Pearson, *NDT & E Int.*, 42 (2009) 16
9. N. Kasai, K. Sekine and H. Maruyama, *J. Jpn. Petro. Inst.*, 46 (2003) 126
10. N. Kasai, Y. Fujiwara, K. Sekine and T. Sakamoto, *NDT & E Int.*, 41 (2008) 525
11. N. Kasai, K. Sekine and H. Maruyama, *J. Jpn. Petro. Inst.,* 47 (2004) 19
12. J. F. Chen, H. S. Bi, Q. Wang, A. Q. Wang, H. Sheng and H. X. Rong, *Advanced Materials Research*, 807-809 (2013) 2652
13. H. S. Bi, Z. L. Li, Y. P. Cheng, Isaac and J. Wang, *Advanced Materials Research*, 694-697 (2013) 1167
14. M. Riahi, H. Shamekh and B. Khosrowzadeh, *Russ. J. Nondestruct*, 44 (2008) 436
15. M. Riahi and H. Shamekh, *Russ. J. Nondestruct,* 42 (2006) 537
16. A. V. Sokolkin, I. Y. Ievlev and S. O. Cholakh, *Russ. J. Nondestruct,* 38 (2002) 113
17. A. V. Sokolkin, I. Y. Ievlev and S. O. Cholakh, *Russ. J. Nondestruct,* 38 (2002) 902
18. N. Kasai, K. Utatsu, S. Park, S. Kitsukawa and K. Sekine, *Corros. Sci.*, 51 (2009) 1679
19. A. Prateepasen, C. Jirarungsatean, P. Tuengsook, S. Lee, J. Lee, I. Park, S. Song and M. Choi, *Advanced Nondestructuve Evaluation*, 321-323 (2006) 545
20. H. S. Bi, Z. L. Li, J. G. Liu, Y. P. Cheng and I. Toku-Gyamerah, *Int J. Electrochem. Sci.*, 10 (2015) 4416
21. A. Prateepasen and C. Jirarungsatian, *Corrosion*, 67 (2011) 056001
22. C. Jirarungsatian and A. Prateepasen, *Corros. Sci.*, 52 (2010) 187
23. K. Darowicki, J. Orlikowski, A. Arutunow and W. Jurczak, *J. Electrochem. Soc.*, 154 (2007) C74
24. S. Krakowiak and K. Darowicki, *J. Solid State Electr.*, 13 (2009) 1653
25. F. Ferrer, T. Faure, J. Goudiakas and E. Andres, *Corros. Sci.,* 44 (2002) 1529
26. M. Fregonese, H. Idrissi, H. Mazille, L. Renaud and Y. Cetre, *Corros. Sci.,* 43 (2001) 627
27. M. Fregonese, H. Idrissi, H. Mazille, L. Renaud and Y. Cetre, *J. Mater. Sci.*, 36 (2001) 557
28. S. Park, S. Kitsukawa, K. Katoh, S. Yuyama, H. Maruyama and K. Sekine, *Mater. Trans.*, 47 (2006) 1240
29. S. Yuyama, M. Yamada, K. Sekine and S. Kitsukawa, *Mater. Eval.*, 65 (2007) 888
30. L. Jaubert, M. Fregonese, D. Caron, F. Ferrer, C. Franck, E. Gravy, P. Labeeuw, H. Mazille and L. Renaud, *Insight*, 47 (2005) 465
31. M. Fregonese, L. Jaubert and Y. Cetre, *Prog. Org. Coat.*, 59 (2007) 239
32. H. Tamura, *Corros. Sci.,* 50 (2008) 1872
33. L. Wang, K. Daub, Z. Qin and J. C. Wren, *Electrochim. Acta*, 76 (2012) 208
34. W. Xu, K. Daub, X. Zhang, J. J. Noel, D. W. Shoesmith and J. C. Wren, *Electrochim. Acta*, 54 (2009) 5727
35. M. Nordsveen, S. Nesic, R. Nyborg and A. Stangeland, *Corrosion*, 59 (2003) 443
36. S. Nesic and K. L. J. Lee, *Corrosion*, 59 (2003) 616

37. A. Gallego, J. Gil, J. Vico, J. Ruzzante and R. Piotrkowski, *Scripta Mater.*, 52 (2005) 1069
38. R. Piotrkowski, E. Castro and A. Gallego, *Mech. Syst. Signal Pr.*, 23 (2009) 432
39. G. Van Dijck and M. Van Hulle, *Sensors*, 11 (2011) 5695
40. A. Gallego, J. F. Gil, E. Castro and R. Piotrkowski, *Surf. Coat. Tech.*, 201 (2007) 4743
41. R. Piotrkowski, A. Gallego, E. Castro, M. T. Garcia-Hernandez and J. E. Ruzzante, *NDT & E Int.*, 38 (2005) 260